

# Spectroscopic distinction between the normal state pseudogap and the superconducting gap of cuprate high $T_c$ superconductors

Li Yu<sup>1,2</sup>, D. Munzar<sup>3</sup>, A.V. Boris<sup>2</sup>, P. Yordanov<sup>2</sup>, J. Chaloupka<sup>3</sup>,

Th. Wolf<sup>4</sup>, C.T. Lin<sup>2</sup>, B. Keimer<sup>2</sup>, and C. Bernhard<sup>1,2</sup>

1.) *University of Fribourg, Department of Physics and Fribourg,*

*Center for Nanomaterials (FriMat), Chemin du Musee 3, CH-1700 Fribourg, Switzerland*

2.) *Max-Planck-Institute for Solid State Research,*

*Heisenbergstrasse 1, D-70569 Stuttgart, Germany*

3.) *Institute of Condensed Matter Physics, Masaryk University, Kotlářská 2, CZ-61137 Brno, Czech Republic*

4.) *Forschungszentrum Karlsruhe, IFP, D-76021 Karlsruhe, Germany*

(Dated: November 30, 2018)

We report on broad-band infrared ellipsometry measurements of the c-axis conductivity of underdoped  $\text{R}\text{Ba}_2\text{Cu}_3\text{O}_{7-d}$  ( $\text{R}=\text{Y}, \text{Nd}, \text{and La}$ ) single crystals. Our data provide a detailed account of the spectral weight (SW) redistributions due to the normal state pseudogap (PG) and the superconducting (SC) gap. They show that these phenomena involve different energy scales, exhibit distinct doping dependencies and thus are likely of different origin. In particular, the SW redistribution in the PG state closely resembles the one of a conventional charge- or spin density wave (CDW or SDW) system.

PACS numbers: 74.72.-h, 78.20.-e, 78.30.-j

It is now widely recognized that the anomalous normal state electronic properties of the cuprate high temperature superconductors (SC) may hold the key for understanding the SC pairing mechanism. The most challenging feature is the so-called pseudogap (PG) phenomenon which prevails in samples that are underdoped with respect to the dome-shaped dependence of the SC critical temperature,  $T_c$ , on hole doping,  $p$  [1, 2]. Here it gives rise to a gap-like depletion of the low-energy charge and spin excitations starting at temperatures well above  $T_c$ . The PG has been identified by several experimental techniques like specific heat [3], angle-resolved photoemission (ARPES) [4], c-axis tunneling [5], and also by infrared (IR) spectroscopy [6, 7, 8]. While these have established some important aspects, like its strong k-space anisotropy [4] or the rapid increase of its magnitude towards the underdoped side [4, 8], the origin of the PG and, in particular, the question of whether it is intrinsic or extrinsic with respect to SC remains heavily debated [2, 3, 9, 10]. Prominent intrinsic theories are the phase fluctuation model where the PG corresponds to a SC state lacking macroscopic phase coherence [11], precursor pairing models where the pair formation occurs at much higher temperature ( $T$ ) than the condensation [12], and the resonating valence bond (RVB) theory [13]. The extrinsic models include numerous conventional and exotic spin- or charge density wave states that are either passive or even competitive with respect to SC [14]. One of the major obstacles in identifying the relevant theory is the lack of a clear spectroscopic distinction between the PG and the SC gap.

In this letter we present broad-band infrared (70-4000  $\text{cm}^{-1}$ ) ellipsometry measurements of the c-axis conductivity for a series of underdoped  $\text{R}\text{Ba}_2\text{Cu}_3\text{O}_{7-\delta}$  ( $\text{R}=\text{Y}, \text{Nd}, \text{La}$ ) single crystals which shed new light on this issue. Our data detail the spectral weight (SW) redistribution

due to the formation of the normal state PG and the SC gap. They highlight significant differences in the related energy scales and their doping dependencies which provide evidence in favor of the extrinsic PG models.

High quality  $\text{R}\text{Ba}_2\text{Cu}_3\text{O}_{7-\delta}$  ( $\text{R}=\text{Y}, \text{Nd}, \text{La}$ ) single crystals were grown with a flux method in Y-stabilized zirconium crucibles under reduced oxygen atmosphere to avoid the substitution of R ions on the Ba site [15]. The oxygen content and the consequent hole doping of the  $\text{CuO}_2$  planes,  $p$ , were adjusted by annealing at appropriate  $T$  in flowing  $\text{O}_2$  gas and subsequent rapid quenching. The quoted  $T_c(\Delta T_c)$  values correspond to the midpoint (10 to 90 % width) of the diamagnetic SC transition as measured by SQUID magnetometry. The doping levels were deduced from the empirical relationship [2]  $p=0.16\pm\sqrt{\frac{1-T_c/T_{c,\text{max}}}{82.6}}$  with  $T_{c,\text{max}} = 92.5, 96$  and  $98$  K for Y, Nd and La, respectively [16]. In agreement with previous reports, we find that the oxygen content needed to obtain a certain value of  $p$  increases with the size of the R ion [16]. The annealing temperatures (in pure  $\text{O}_2$  gas), the resulting oxygen deficiencies,  $\delta$ , and the  $T_c$  values at  $p \approx 0.12$  are  $570$  °C,  $\delta \approx 0.2$ ,  $T_c=82(1)$  K for Y-123,  $440$  °C,  $\delta \approx 0.1$ ,  $T_c=85(2)$  K for Nd-123, and  $310$  °C,  $\delta \approx 0$ ,  $T_c=87(2)$ K for La-123.

The ellipsometry experiments were performed with a home-built ellipsometer attached to a Bruker Fast-Fourier spectrometer at the infrared (IR) beamline at the ANKA synchrotron at FZ Karlsruhe, D for the range of  $70\text{-}700$   $\text{cm}^{-1}$  and with a corresponding laboratory-based setup at  $400\text{-}4000$   $\text{cm}^{-1}$  [17]. Ellipsometry directly measures the complex dielectric function,  $\tilde{\epsilon} = \epsilon_1 + i\epsilon_2$ , and the related optical conductivity  $\tilde{\sigma}(\omega) = i \cdot \omega (1 - \tilde{\epsilon}(\omega))$ , without a need for a Kramers-Kronig analysis [18]. It is furthermore a self-normalizing technique that enables a very accurate and reproducible measurement of  $\tilde{\epsilon}$  and, in par-

ticular, of its  $T$ -dependent changes. We note that thanks to the large probe depth of the infrared radiation ( $\sim 1 \mu\text{m}$ ) which ensures the bulk nature of the observed phenomena, the high energy resolution, and the accuracy in the determination of the optical constants which enables the application of powerful sum rules, this technique provides important complementary information with respect to other techniques like ARPES or tunneling.

Figure 1 summarizes our data of the c-axis optical conductivity,  $\sigma_{1c}(\omega)$ , for the underdoped ( $p \approx 0.12$ )  $\text{NdBa}_2\text{Cu}_3\text{O}_{6.9}$  crystal. Representative spectra in the PG and the SC states are shown in Fig. 1a and 1b, respectively. The spectral shape of the  $T$ -dependent changes is detailed in Fig. 1c in terms of the conductivity difference spectra,  $\Delta\sigma_{1c} = \sigma_{1c}(T) - \sigma_{1c}(300 \text{ K})$ . The  $T$ -dependence of the integrated spectral weight,  $\text{SW}_\alpha^\beta = \int_\alpha^\beta \sigma_{1c}(\omega) d\omega$ , is given in Figs. 1d-1f for representative integration limits.

First, we focus on the spectral changes due to the normal state PG which gives rise to a gap-like suppression of the low frequency part of  $\sigma_{1c}(\omega)$  below an onset temperature,  $T^* > T_c$ . From the  $T$ -dependence of  $\text{SW}_{0+}^{800}$  in Fig. 1d we estimate  $T^* \approx 220 \text{ K}$ . Figure 1a shows the corresponding crossing point in  $\sigma_{1c}(\omega, T)$  at  $\omega_{PG}^* \approx 700 \text{ cm}^{-1}$  which separates the low frequency region, where  $\sigma_{1c}$  undergoes a gap-like suppression, from the high frequency one, where  $\sigma_{1c}$  exhibits a corresponding increase. In classical spin- or charge density wave (SDW or CDW) systems this crossing is determined by the magnitude of the gap, i.e.  $\hbar\omega^* \approx 2\Delta$  [19]. In analogy, we use the same relationship to estimate the magnitude of the PG, i.e.  $\hbar\omega_{PG}^* \approx 2\Delta^{PG}$ . Even though the origin of the PG remains unknown, we still believe that this estimate yields a reasonable value for  $\Delta^{PG}$  and especially for its variation with doping. Apart from some controversy regarding the determination of the magnitude of  $\omega_{PG}^*$ , which requires a very precise measurement of  $\Delta\sigma_{1c}(T)$ , our data agree well with previous reports of FIR reflectivity [1, 6, 7] and ellipsometry [8, 20]. In addition, our new broad-band ellipsometry data answer the long standing question of where the SW is accumulated that is removed from the FIR range (at  $\omega < \omega_{PG}^*$ ). Note that the SW, if integrated to a sufficiently high frequency, should be conserved and thus  $T$  independent (the so-called SW sum rule). Our data establish that the gap like suppression of  $\sigma_{1c}(\omega < \omega_{PG}^*)$ , is balanced by the corresponding increase of  $\sigma_{1c}(\omega > \omega_{PG}^*)$  which yields a broad MIR band that starts right at the gap edge and extends to about  $3500 \text{ cm}^{-1}$ . The amount of transferred normal state SW is  $\sim 13000 \Omega^{-1}\text{cm}^{-2}$ . The SW balance is evident from the smooth evolution of  $\text{SW}_{0+}^{4000}$  which, unlike  $\text{SW}_{0+}^{800}$ , does not exhibit a sizeable decrease below  $T^*$ . The remaining decrease of  $\text{SW}_{0+}^{4000}$  (mostly above 200 K) is actually unrelated to the PG phenomenon. It occurs for all doping levels both for the c-axis (data for overdoped samples are not shown here) and for the in-plane response [21]. Figure 1c also shows that the related  $\Delta\sigma_{1c}(\omega)$  spectra are

rather different, i.e.  $\Delta\sigma_{1c}(\omega)$  is always positive at  $T > T^*$  while at  $T_c < T < T^*$  it exhibits a sign change at  $\omega_{PG}^*$ . Notably, the spectral shape of the PG-related SW redistribution closely resembles the one of a conventional charge- or spin density wave (CDW or SDW) system which is described in Ref. [19].

Next we discuss what impact the SC transition has on the PG-related SW redistribution, in particular, on the broad MIR band. We focus here on the data at  $\omega > 1600 \text{ cm}^{-1}$  which are not affected by the much narrower and SC-induced band near  $1000 \text{ cm}^{-1}$  which is unrelated to the PG phenomenon as discussed below. In the first place, Fig. 1b shows that  $\sigma_{1c}(\omega > 1600 \text{ cm}^{-1})$  undergoes hardly any noticeable changes below  $T_c$ . Any SC induced modification of the broad MIR band therefore must be fairly small. Nevertheless, a weak but yet significant impact of SC on the MIR band is apparent from the  $T$  dependence of  $\text{SW}_{1600}^{4000}$  in Fig. 1f. Its rapid increase below  $T^*$  is suddenly interrupted near  $T_c$  followed by a saturation or even a minor decrease below  $T_c$ . We have confirmed this trend for several underdoped Y-123 crystals (data are not shown here). Notably, a similar behavior was previously observed in the A-15 compounds where the onset of SC arrests the anomalous softening of a phonon mode that is associated with a CDW-like instability [22]. Just like this observation had inspired the classical theoretical work on competing CDW (SDW) and SC order parameters [23], we hope that our new results will motivate further theoretical studies concerning the SW redistributions in the context of the various proposed PG models. We also note that our data seem to provide a challenge to the phase fluctuation models. Naively one would expect here that a significant part of the SW of the broad MIR band is transferred back to low energies and joins the SC condensate once the phase fluctuations diminish below  $T_c$ . Not to be misunderstood, we do not argue that our data provide evidence against the existence of precursor SC fluctuations, which are meanwhile well established. However, our data suggest that these SC fluctuations are not causing the normal state PG phenomenon. Instead they may well be a consequence of the PG-like suppression of the low energy SW and thus of the SC condensate density. The minor decrease of  $\text{SW}_{0+}^{4000}$  below about 120 K in Fig. 1e may well be a signature of these precursor SC fluctuations.

Finally, we note that our data confirm previous reports [24] that the SW transfer in the SC state involves an anomalously high energy scale. This is evident from Fig. 1e where  $\text{SW}_0^{4000}$ , including the SW of the SC delta function at the origin,  $\text{SW}^\delta$  (solid blue circles, as deduced by fitting a Drude-Lorentz model to the complex dielectric function), apparently exhibits an anomalous increase below  $T_c$ . The comparison with the estimated trend based on a power law fit to the normal state data, as shown by the red thin line in Fig. 1e, suggests that about 20 % of  $\text{SW}^\delta$  originates from the high frequency range of  $\omega > 4000 \text{ cm}^{-1}$ . Notably, our data suggest that this anomalous contribution to  $\text{SW}^\delta$  does not arise from a partial rever-

sal of the PG-related SW transfer which is confined to the region below  $4000 \text{ cm}^{-1}$  as shown above.

In Fig. 2 we compare the doping dependencies of the spectral gaps in the PG and SC states. In analogy to the PG case, we estimate the magnitude of the SC gap,  $\Delta^{SC}$ , as  $2\Delta^{SC} \approx \hbar\omega_{SC}^*$ , where  $\omega_{SC}^*$  is the frequency of the crossing point as shown in Figs. 1b and 2c. A justification for this approach is given in the next paragraph. Figure 2a displays the resulting phase diagram of  $\Delta^{PG}$  and  $\Delta^{SC}$  as obtained for a series of strongly to very weakly underdoped Y-123 single crystals. The evaluation of  $\omega_{PG}^*$  and  $\omega_{SC}^*$  is detailed in Figs. 2b and 2c, respectively. In the first place, Fig. 2a shows that  $\Delta^{PG}$  exhibits a considerably stronger doping dependence than  $\Delta^{SC}$ . Notably, there is a crossing point around  $p \approx 0.12$  which separates regions of  $\Delta^{PG} > \Delta^{SC}$  ( $\Delta^{PG} < \Delta^{SC}$ ) at low (high) doping. We note that the finding of  $\Delta^{PG} > \Delta^{SC}$  for  $p < 0.12$  has important implications, in particular, it contrasts with the expectation that the PG and the SC gap add to form the measured spectroscopic gap, i.e. that  $\Delta = \sqrt{\Delta_{PG}^2 + \Delta_{SC}^2}$ . The observation of  $\Delta^{PG} > \Delta^{SC}$  may be accounted for in terms of a spatial separation of the two gaps. However, our optical data can not tell whether this separation takes place in real or in k-space. Nevertheless, the latter possibility is indeed suggested by recent ARPES data [25]. Furthermore, while we cannot follow the evolution of  $\Delta^{PG}$  beyond optimum doping where  $T^* \leq T_c$ , the linear extrapolation of our data suggests that the PG vanishes much earlier than  $\Delta^{SC}$  at a critical doping of  $p_{crit} \approx 0.19 - 0.2$  which agrees well with previous reports of a sudden change in the electronic properties [2, 20]. Accordingly, our data once more favor the extrinsic PG models, in particular, they suggest that  $\Delta^{PG}$  and  $\Delta^{SC}$  do not merge on the overdoped side as predicted by the intrinsic models.

We return now to the discussion of the SC-induced mode near  $1000 \text{ cm}^{-1}$  mode and the relationship between  $\hbar\omega_{SC}^*$  and  $2\Delta^{SC}$ . Figure 3 shows data for a series of similarly underdoped ( $p \approx 0.12$ ) R-123 with R=Y, Nd, and La crystals which establish that the intensity of the  $1000 \text{ cm}^{-1}$  strongly depends on the size of the ionic radius of the R ion and the related strength of the electronic bilayer coupling. The expected correlation between the R ionic size which increases from  $1.019 \text{ \AA}$  for  $\text{Y}^{3+}$ , to  $1.109 \text{ \AA}$  for  $\text{Nd}^{3+}$ , and  $1.16 \text{ \AA}$  for  $\text{La}^{3+}$  [16] and the bilayer coupling is

confirmed by recent ARPES measurements on the same samples (private communication with S. Borisenko) and also by the sizeable red shift of the so-called transverse Josephson plasma resonance (t-JPR) mode [26] near  $500 \text{ cm}^{-1}$ . Here we only mention two possible interpretations of the  $1000 \text{ cm}^{-1}$  mode. Firstly, it may correspond to an interband (bonding-antibonding) pair-breaking peak whose coherence factor decreases with decreasing bilayer coupling [27]. This appealing interpretation is still speculative because final state interactions have not been taken into account in the calculations of Ref. [27]. Alternatively, the mode could be due to final states involving two Bogolyubov quasiparticles and a bosonic mode (e.g. the neutron resonance), an interpretation similar to that of the well known maximum around  $1000 \text{ cm}^{-1}$  in the SC state in-plane conductivity [7]. Irrespective of the outcome of this ongoing work, we note that according to both interpretations the maximum is located a few tens meV above the SC gap, suggesting that the difference between  $\Delta^{SC}$  and the true single particle gap is small. This conclusion is furthermore supported by the data of the La-123 crystal which are shown in Fig.4. Here the  $1000 \text{ cm}^{-1}$  mode is absent and  $2\Delta^{SC}$  can be estimated as  $\hbar\omega_{SC}^*/2$  [28], where  $\omega_{SC}^*$  is the frequency of the shoulder feature as marked by the cyan arrow. Notably, the obtained value of  $2\Delta^{SC} \approx 800 \text{ cm}^{-1}$  compares rather well with the ones of  $2\Delta^{SC} \approx 780 \text{ cm}^{-1}$  in Y-123 and  $2\Delta^{SC} \approx 860 \text{ cm}^{-1}$  in Nd-123. Another interesting trend occurs for the PG magnitude of  $2\Delta^{PG} \approx 1200 \text{ cm}^{-1}$  in La-123 which is almost doubled as compared to the one in Y-123 and Nd-123. At present we do not know whether this trend reflects a strong dependence of the PG correlations on the electronic bilayer coupling or rather a sensitivity to structural disorder, e.g. in the Ba-O layer, which is likely enhanced in La-123. This issue deserves further investigation and may well open up new possibilities for distinguishing between the PG phenomenon SC gap with other spectroscopic techniques.

We acknowledge financial support by the Schweizer Nationalfonds (SNF) by grant 200021-111690/1 and the Deutsche Forschungsgemeinschaft (DFG) by grant BE2684/1-1 in FOR538. D.M. and J.C were supported by the Ministry of Education of CR (MSM0021622410). We are indebted to Y.L. Mathis for technical support at ANKA.

- 
- [1] T. Timusk and B. Statt, Rep. Prog. Phys. **62**, 61 (1999).  
[2] J.L. Tallon, J.W. Loram, Physica **C 349**, 53 (2001).  
[3] J.W. Loram, K.A. Mirza, J.R. Cooper, and W.Y. Liang, Phys. Rev. Lett. **71**, 1740 (1993).  
[4] A.G. Loeser *et al.*, Science **273**, 325 (1996).  
[5] V.M. Krasnov, A. Yurgens, D. Winkler, P. Delsing, and T. Claeson, Phys. Rev. Lett. **84**, 5860 (2000).  
[6] C.C. Homes, T. Timusk, R. Liang, D.A. Bonn, and W.N.Hardy, Phys. Rev. Lett. **71**, 1645 (1993).  
[7] D.N. Basov and T. Timusk, Rev. Mod. Phys. **77**, 721 (2005).  
[8] C. Bernhard *et al.*, Phys. Rev. **B 59**, R6631 (1999); *ibid* Phys. Rev. Lett. **80**, 1762 (1998).  
[9] M. Kugler, O. Fischer, C. Renner, S. Ono, and Y. Ando, Phys. Rev. Lett. **86**, 4911 (2001).  
[10] N. Miyakawa, Physica **C 364**, 475 (2001).  
[11] V.J. Emery and S.A. Kivelson, Nature **374**, 434 (1995).  
[12] I. Kosztin, Q. Chen, Y.J. Kao, and K. Levin, Phys. Rev. **B 61**, 11662  
[13] P.W. Anderson, J. Phys. Condensed Mat. **16**, R755

- (2004).
- [14] A.V. Chubukov and J. Schmalian, Phys. Rev. **B 57**, R11085 (1998); C.M. Varma, Phys. Rev. Lett. **83**, 3538 (1999).
  - [15] S.I. Schlachter *et al.*, Int. J. Modern Phys. **B 14**, 3673 (2000).
  - [16] G.V.M. Williams and J.L. Tallon, Physica **C 258**, 41 (1996).
  - [17] C. Bernhard, J. Humlicek, and B. Keimer, Thin Solid Films **455-456**, 143 (2004).
  - [18] R.M.A. Azzam and N.H. Bashara, *Ellipsometry and Polarized Light* (North-Holland, Amsterdam, 1977).
  - [19] G. Grüner, in *Density Waves in Solids*, Addison Wesley, Reading, MA 1994.
  - [20] A.V. Pimenov *et al.*, Phys. Rev. Lett. **94**, 227003 (2005).
  - [21] M. Ortolani, P. Calvani, and S. Lupi, Phys. Rev. Lett. **94**, 067002 (2005).
  - [22] L.R. Testardi, Rev. Mod. Phys. **47**, 637 (1975).
  - [23] C.A. Balseiro and L.M. Falicov, Phys. Rev. **B 20**, 4457 (1979).
  - [24] D.N. Basov *et al.*, Science **283**, 49 (1999); D.N. Basov *et al.*, Phys. Rev. **B 63**, 134514 (2001).
  - [25] K. Tanaka *et al.*, cond-mat/0612048.
  - [26] D. van der Marel and A. Tsvetkov, Czech. J. Phys. **46**, 3165 (1996); D. Munzar *et al.*, Solid State Commun. **112**, 365 (1999); M. Grüninger, D. van der Marel, A.A. Tsvetkov, and A. Erb, Phys. Rev. Lett. **84**, 1575 (2000).
  - [27] D. Munzar, J. Phys. Chem. Solids **67**, 308 (2006).
  - [28] P.J. Hirschfeld, S.M. Quinlan, D.J. Scalapino, Phys. Rev. **B 55**, 12742 (1997).

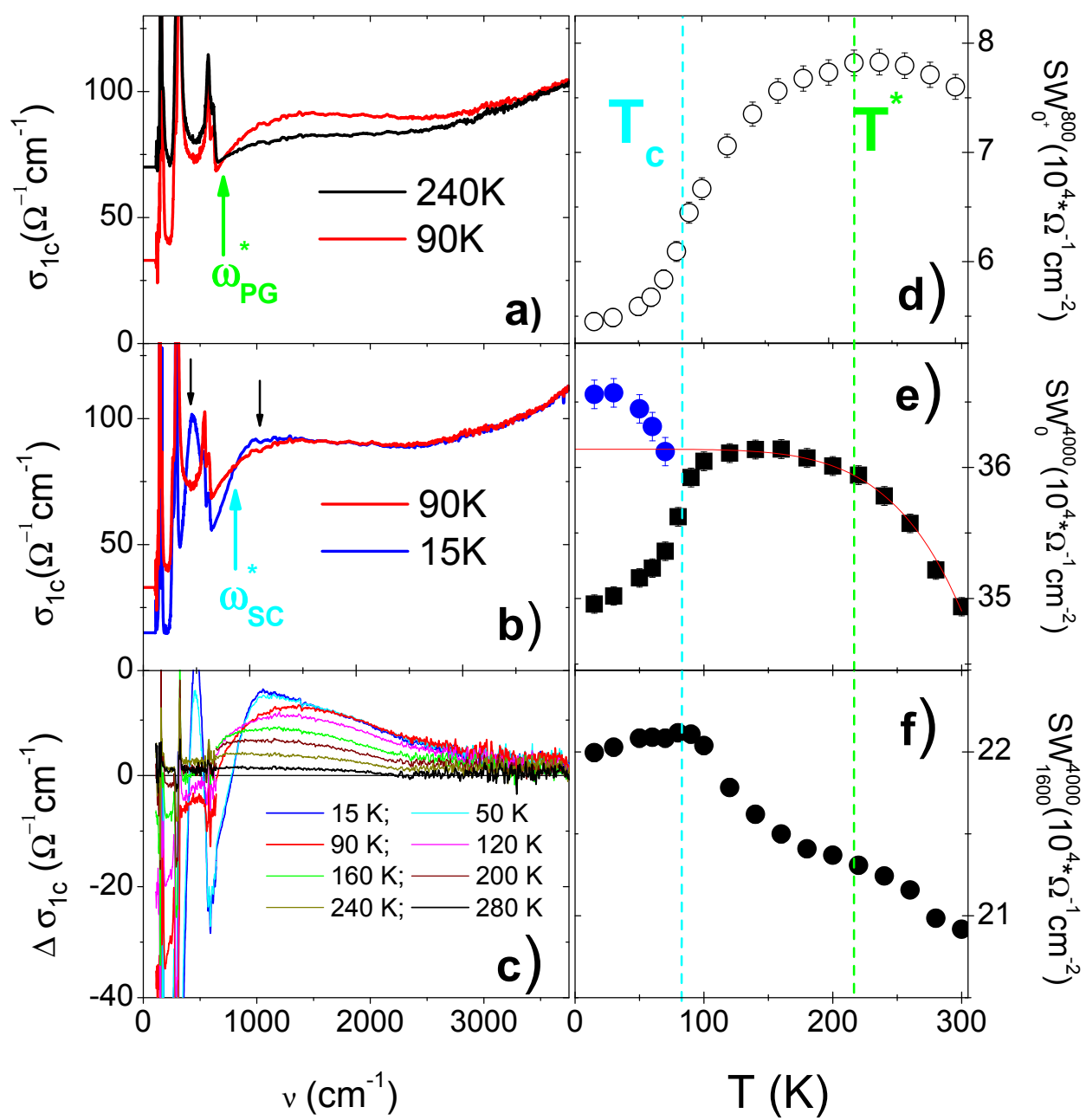
Figure 1: Infrared c-axis conductivity,  $\sigma_{1c}(\omega)$ , of underdoped NdBa<sub>2</sub>Cu<sub>3</sub>O<sub>6.9</sub>. Shown are representative spectra for (a) the PG state, (b) the SC state, and (c) the  $T$ -difference,  $\Delta\sigma_{1c} = \sigma_{1c}(T) - \sigma_{1c}(300\text{ K})$ . Green

(cyan) arrows mark the crossing points at  $\omega_{PG}^*$  ( $\omega_{SC}^*$ ). Also shown is the  $T$ -dependence of the integrated spectral weight,  $SW_{\alpha}^{\beta} = \int_{\alpha}^{\beta} \sigma_{1c}(\omega) d\omega$ , for (d)  $\alpha=0^+$  and  $\beta=800\text{ cm}^{-1}$  (regular part), (e)  $\alpha=0$  and  $\beta=4000\text{ cm}^{-1}$  (black squares show the regular part while blue circles include the contribution of the SC delta function,  $SW^{\delta}$ ), and (f)  $\alpha=1600$  to  $\beta=4000\text{ cm}^{-1}$ . The red line in (e) shows a fit to the normal state data with the function  $SW(T) = SW_0 \left(1 - \left(\frac{T}{\Theta}\right)^{\beta}\right)$ .

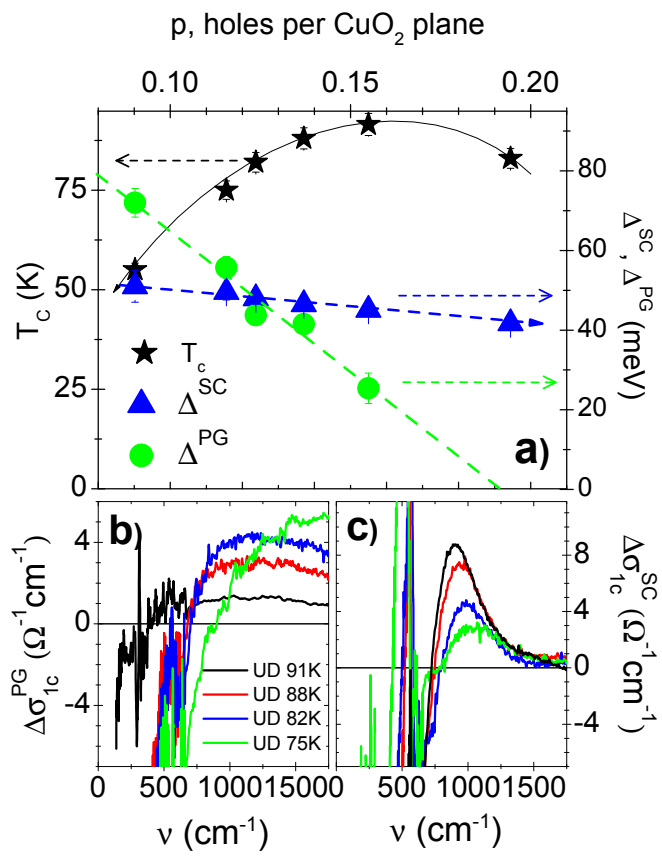
Figure 2: (a) Phase diagram of Y-123 showing the doping dependencies of the critical temperature,  $T_c$  (black stars), the PG magnitude,  $\Delta^{PG}$  (green circles), and the SC gap,  $\Delta^{SC}$  (blue triangles). The dashed green (cyan) line shows a linear extrapolation of  $\Delta^{PG}$  ( $\Delta^{SC}$ ) towards the overdoped side. (b) and (c) Conductivity difference spectra,  $\Delta\sigma_{1c}^{PG} = \sigma_{1c}(T \approx T_c) - \sigma_{1c}(T \approx T^*)$  and  $\Delta\sigma_{1c}^{SC} = \sigma_{1c}(10K) - \sigma_{1c}(T \approx T_c)$ , showing the changes due to the PG and the SC gap, respectively. Some sharp features due to a  $T$ -dependent shift of phonon modes have been removed for clarity.

Figure 3: (a)-(c) Infrared c-axis conductivity for R-123 (R=Y, Nd and La) with  $p \approx 0.12$ . Black dotted (solid) arrows mark the transverse Josephson plasma mode (mode near  $1000\text{ cm}^{-1}$ ). (d) Corresponding difference spectra,  $\Delta\sigma_{1c} = \sigma_{1c}(10K) - \sigma_{1c}(90K)$ .

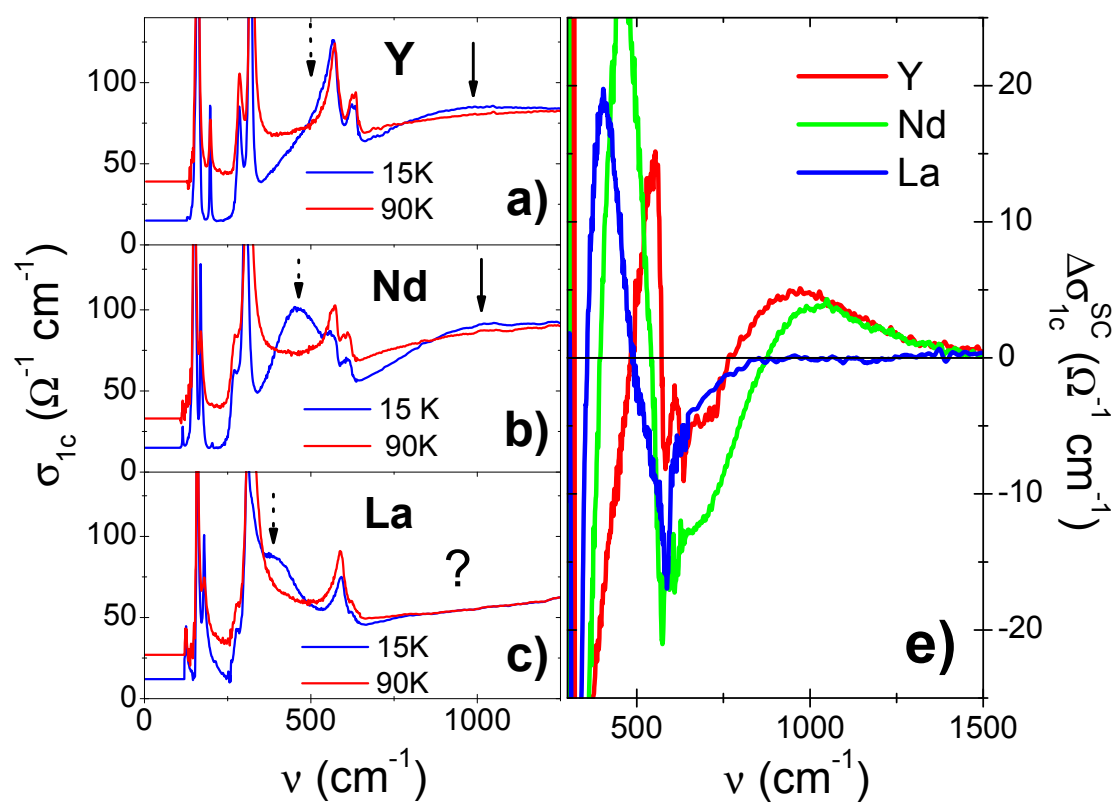
Figure 4: Infrared c-axis conductivity,  $\sigma_{1c}(\omega)$ , of underdoped LaBa<sub>2</sub>Cu<sub>3</sub>O<sub>7</sub> with  $T_c = 87(2)\text{ K}$ . Green and cyan arrows mark the onset of the PG and the SC gap, respectively.



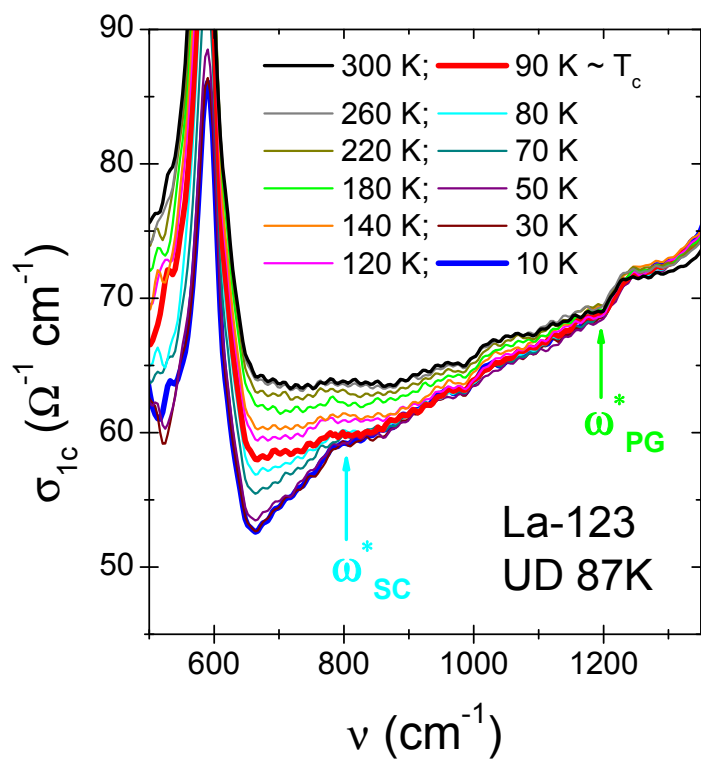
Yu-Fig.1



Yu-Fig. 2



Yu-Fig. 3



Yu-Fig. 4